Наносистеми, наноматеріали, нанотехнології
Nanosistemi, Nanomateriali, Nanotehnologii
2022, т. 20, № 1, сс. 195–205

PACS numbers: 61.05.cp, 68.37.Hk, 68.37.Ps, 78.30.Jw, 79.60.Fr, 82.35.-x, 82.80.Pv

Synthesis and Characterisation of Poly(2-Formylpyrrole) (PFPy) by Acids Catalysis and Study of Its Particles' Size

Ahmad Al-Hamdan[1], Ahmad Al-Falah[2], Fawaz Al-Deri[1], and Ibrahim Al-ghoraibi[3]

[1]*Department of Chemistry*
Damascus University,
Damascus, Syria
[2]*Department of Chemistry and Faculty of Pharmacy,*
Arab International University (AIU),
Damascus, Syria
[3]*Department of Physics,*
Damascus University,
Damascus, Syria

In this paper, poly(2-formyl pyrrole) (PFPy) is synthesized using hydrochloric acid as catalyst in alcohol. PFPy is dark-green very fine powder. Then, the polymer forms glass substrate in the reaction mixture. The resulting polymer is characterized by FTIR, EDX and XPS to determine the polymer structure. The polymer is scanned by scanning electron microscope (SEM), and its film is investigated by atomic force microscope (AFM) for its morphological properties. We found the polymer consisting of spherical particles with a rough surface (with average diameters of 430 nm), and they form clusters. We propose a method for calculation of particles' size depending on the crystals' size (by means of the Scherrer equation) and percentage of crystallization of polymer from XRD analysis. The average particles' size is of 336.7 nm. The particles' size in this method may be closer to reality because the XRD analysis includes a large number of particles, and it is not optional as based on the SEM and AFM characterization.

У цій роботі полі(2-форміловий пірол) (ПФП) синтезується з використанням соляної кислоти в якості каталізатора у спирті. ПФП є темно-зелений дуже тонкоподрібнений порошок. Потім полімер утворює скляну підкладинку в реакційній суміші. Одержаний полімер характеризується інфрачервоною спектроскопією на основі Фур'є-перетвору, методами енергодисперсійної рентґенівської спектроскопії та рентґенівської фотоелектронної спектроскопії для визначення полімерної структури. Полімер сканується сканувальним електронним мікроскопом (СЕМ),

а його плівка досліджується атомно-силовим мікроскопом (АСМ) на предмет його морфологічних властивостей. Ми виявили полімер, що складається зі сферичних частинок із шерсткою поверхнею (із середнім діяметром у 430 нм), і вони утворюють скупчення. Запропоновано методу розрахунку розміру частинок залежно від розміру кристалів (за допомогою Шеррерового рівняння) та відсотка кристалізації полімеру за даними рентґеноструктурної аналізи. Середній розмір частинок становить 336,7 нм. Розмір частинок у цій методі може бути ближче до реальности, оскільки рентґеноструктурна аналіза включає велику кількість частинок, та вона не є необов'язковою, оскільки базується на характеризації через СЕМ та АСМ.

Key words: polymerization, acid catalysis, XRD, particles' size, polyformyl pyrrole.

Ключові слова: полімеризація, кислотна каталіза, рентґенівська дифракція, розмір частинок, поліформіловий пірол.

(Received 27 March, 2021; in revised form, 8 April, 2021)

1. INTRODUCTION

Conductive polymers were discovered in the mid of 20th century; this was a turning point in the scientific world due to their wide range of applicability [1]. Recently, conducting polymers are used in sensors [2, 3], biosensors [3], capacitors [4], solar cells [5], optical displays [6], and light emitting diodes [7], as rechargeable batteries [8], enzyme immobilization matrices [9], membranes [10], gas separation membranes [11] and electrochromic devices [12]. Conductive polymers were used as thin films for most of their applications. In recent years, synthesis and characterization of polymers containing heteroaromatic rings [13] such as pyrrole, furan and thiophene [14] have been extensively studied because of their potential in advanced optoelectronic applications [13]. Polypyrrole (PPy) and its derivatives are the most widely studied conductive polymers due to the easily oxidizable monomer in aqueous solution [15], the high electrical conductivity, good electrochemical properties, thermal stability [16] and the high mechanical strength, which is easily generated both chemically and electrochemically [17]. Intrinsic properties of polypyrrole including environmental stability, good redox and conductivity behaviour [18] have many applications, including batteries, electrochemical sensors and biosensors [19], conductive textiles and fabrics, drug delivery systems and mechanical actuators [20]. Polypyrrole is electrochemically driven and can be constructed in linear or bending (bilayer) actuators. [21] Poly(2-formylpyrrol) was synthesized by addition of thionylchloride to its solution in tet-

rachlorocarbon [22]. The 2-formylpyrrole can polymerize in acid without an oxidizing agent. Poly(2-formylpyrrole) was synthesized using acidic catalyst in alcohol. The prepared polymer was characterized by FTIR, XPS, EDX, SEM and EIS technique.

2. EXPERIMENTAL

2.1. Materials

Pyrrole-2-carboxaldehyde 98% sigma, hydrochloric acid 35.5% sigma, sulfuric acid 98% sigma acetic acid, trichloroacetic acid sigma, formic acid sigma.

2.2. Measurements

Poly(2-formylpyrrole) was characterized with FTIR (JASCO FT/IR model M4100) spectrophotometer between 4000 and 400 cm^{-1}. Surface morphologies were examined with SEM, EDX and XPS (TESCAN model MIRA3), XRD (Philips, model:PW1370, Cu(0.154056 nm) step size 0.05 deg.) and AFM (Nanosurf model:eseyscan2).

2.3. Synthesis

The 2-formyl pyrrole (10 mmol, 0.97 g) was dissolved in the alcohol (25 ml); then hydrochloric acid 35.5% (10 ml) was added. Mixture solution was placed at room temperature for 48 h. Colour of reaction solution changed to yellow one and then to black one. Then, the polymer precipitates and forms on the walls of the reaction vessel and any substrate (*e.g.*, glass) in the reaction mixture. Formed precipitate was collected by decantation; KOH (5%) solution was added, and mixture was boiled for several minutes. The precipitate was filtered and washed with distilled water and, then, alcohol each one several times and dried at 105°C for 48 hours. It was kept for study later on.

3. RESULTS AND DISCUSSION

3.1. FTIR Analysis

FTIR spectrum of solid content of the reaction was recorded after 2, 7, 15, 30 min and 48 h (polymer). Figure 1 shows FTIR spectrum for monomer and solid content of the reaction at several reaction times. For monomer (Fig. 1, *a*), the peak at 3441 cm^{-1} was related

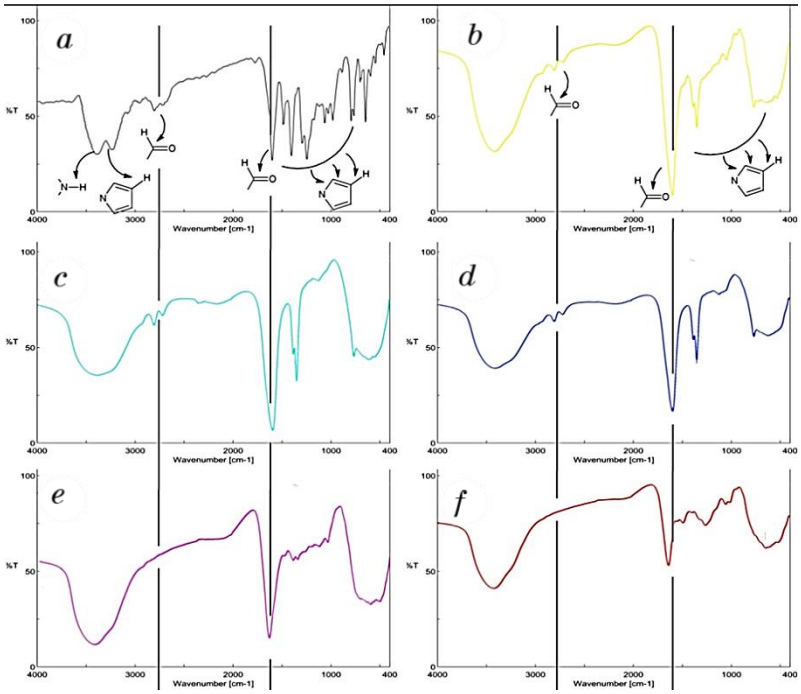

Fig. 1. FTIR spectrum: *a*—monomer; *b*—solid content of the reaction after 2 min; *c*—after 7 min; *d*—after 15 min; *e*—after 30 min; *f*—polymer.

to N–H in pyrrole rings, absorption bands at 3230 cm^{-1} were due to aromatic C–H, peaks about 2757 cm^{-1} are attributed to C–H aldehyde, peak at 1667 cm^{-1} was related to C=O aldehyde, and the peaks between 1500 cm^{-1} to 1000 cm^{-1} were due to C=C in pyrrole ring and C–H out of plane. Solid content of the reaction after 2, 7, 15 and 30 min (Fig. 1, *b*, *c*, *d* and *e*, respectively) have wide peak at 3512 cm^{-1}, which was due to humidity. Most peaks were shifted because of polymerization. The peak at 3441 cm^{-1} for monomer is masque by the peak at 3512 cm^{-1} because water confinement within the polymer structure. Also, the peak at 1667 cm^{-1} in monomer spectra become weaker and was shifted to 1671 cm^{-1}, 1675 cm^{-1}, 1678 cm^{-1}, 1680 cm^{-1}, 1685 cm^{-1} for 2, 7, 15, 30 min and polymer, respectively. This shows that polymerization reaction is happened on aldehyde group. Peaks in the fingerprint region after polymerization were become weaker and less intense.

3.2. XPS Analysis

X-ray photoelectron spectroscopy (XPS) is an excellent technique

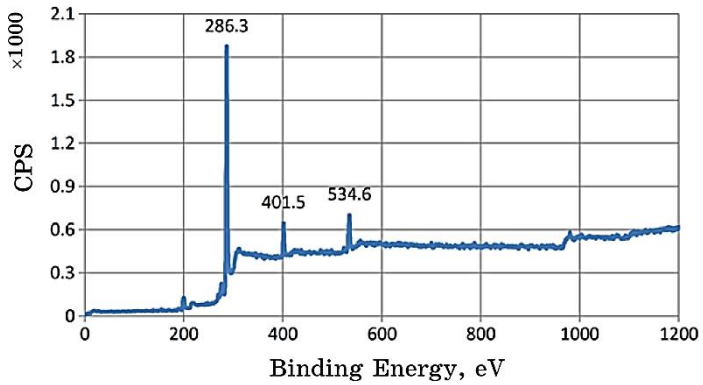

Fig. 2. X-ray photoelectron spectroscopy for PFPy.

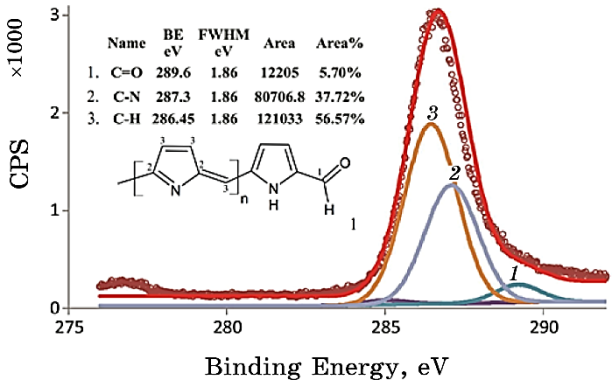

Fig. 3. C1*s* spectra with typical peaks.

for analysing the top of 5–10 nm of a surface. Figure 2 shows the x-ray photoelectron spectroscopy for polymer PFPy. XPS spectra had three peaks at 534.6, 401.5 and 286.3 eV, which were due to O1*s*, N1*s* and C1*s*, respectively. This shows that the polymer make up carbon, oxygen and nitrogen.

Figure 3 shows the analysis of C1*s* peak. From Figure 3, carbon atoms in polymer were of three kinds: C=C–H (286.45) 56.57%, C–N (287.3) 37.72%, C=O (289.6) 5.7%. This result corresponds to number of atoms in the formula.

3.3. EDX Analysis

EDX is used to determine the relative composition of the elements on a surface. Table 1 shows EDX analysis for three areas of polymer surface. This table shows disproportionate relative composition due

TABLE 1. EDX analysis for three areas of polymer surface.

area 3			area 2		area 1		Element
Element C	Atomic, %	wt.%	Atomic, %	wt.%	Atomic, %	wt.%	
100.0%	70.4	64.8	74.6	68.5	66.2	61.2	C
19.1%	13.5	14.5	8.8	9.4	18.2	19.6	N
22.0%	15.5	19.0	15.4	18.8	15.6	19.2	O
0.9%	0.6	1.7	1.2	3.3	0.0	0.0	Cl
	100.0	100.0	100.0	100.0	100.0	100.0	Total

to the inaccuracy of the EDX analysis. The polymer contains carbon 70.42%, nitrogen 13.48% and oxygen 15.02%. The rate N/C is of about 19.1% (one nitrogen atom for five carbon atoms). This is according with polymer structure. The oxygen rate is more than expected because of the water confinement within the polymer structure.

3.4. Scanning Electron Microscopy

The morphology of poly(2-formylpyrrole) particles was studied using scanning electron microscope. Figure 4 shows the photo of its scanning electron microscopy (SEM). The polymer consists of spherical nanoparticles, which were merged together to be cluster. The particles in the cluster have rough surface and average size of about 438 nm.

3.5. X-Ray Diffraction (XRD)

The crystal structures of PFPy were characterized by XRD analysis. Figure 5, *a* shows the XRD pattern of PFPy. The broad peaks below the baseline are mainly due to the scattering from PFPy chains at the interplanar spacing and indicate a typical form of amorphous polymer [23]. To determine the crystalline percentage $P_{cry}\%$, it is essential to deconvolute the XRD spectra of the samples to find the area of the amorphous and crystalline peaks [24]. The $P_{cry}\%$ was calculated using Equation from [25, 26]:

$$P_{cry}\% = \frac{A_{cry}}{A_{cry} + A_{Amo}} \times 100\,, \tag{1}$$

where A_{cry} and A_{Amo} are the area of crystalline peaks and the area of amorphous ones, respectively [26]. The crystalline percentage $P_{cry}\%$

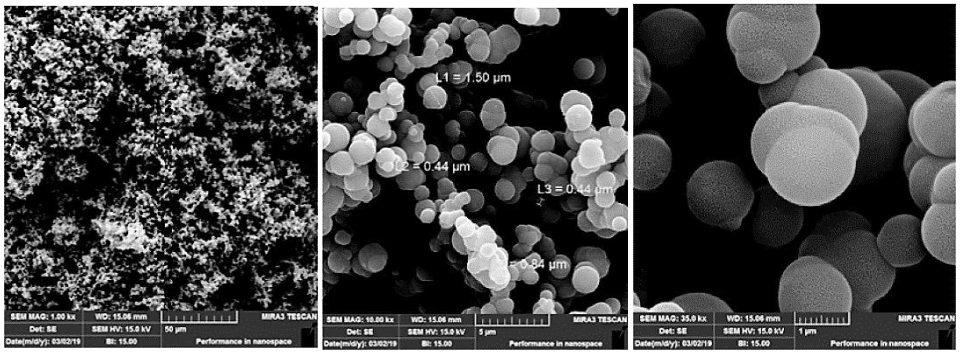

Fig. 4. Photo of the scanning electron microscopy (SEM) for polymer.

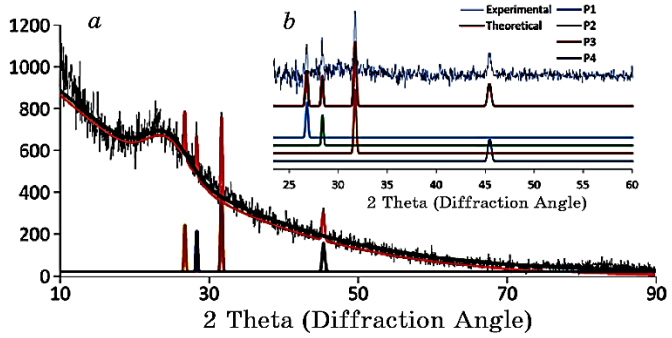

Fig. 5. X-ray diffraction (XRD) for polymer.

was of about 1.46%. Figure 5, *b* shows the XRD pattern of PFPy for crystalline part. If we check the main peaks of the XRD patterns carefully, the peaks situate at 26.81, 28.42, 31.75 and 45.45° giving *d* spacing of 0.333, 0.314, 0.282 and 0.199 nm, respectively [27].

Table 2 shows the percentage areas of crystalline peaks, particles' size and *d* spacing for polymer from XRD pattern.

The polymer particles are formed during the deposition of the polymer from the solution; in the beginning, crystals are formed of several polymer chains, and then, particles are randomly gathered to configure particles (Fig. 6).

In the polymer particle, percentage of the crystals can be given by

$$P_{cry}\,\% = \frac{m_{cry}}{m_{tot}} \times 100\,. \qquad (2)$$

The density of polymer is same for crystal and amorphous parts. So, Eq. (2) can be written as follows:

TABLE 2. Percentage areas of crystalline peaks and their parameters.

Peak No.	2 theta, °	*A*, %	*FMW*, rad	Particles' size, nm	*d* spacing, nm
P1	26.81	0.30%	0.00240	58.61	0.333
P2	28.42	0.24%	0.00204	69.49	0.314
P3	31.75	0.62%	0.00347	41.05	0.282
P4	45.45	0.30%	0.00290	51.28	0.199

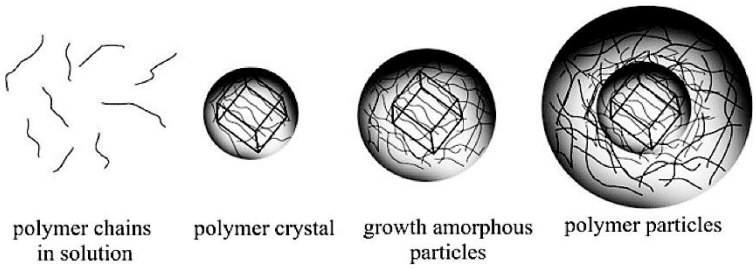

Fig. 6. Growth of polymer particles on its crystal.

$$P_{cry}\% = \frac{v_{cry}}{v_{tot}} \times 100 = \frac{r_{cry}^3}{r_{tot}^3} \times 100\,. \tag{3}$$

For i^{th} crystal, its diameter is D_i and percentage $P_i\%$ based on Eq. (2) can be written as follows:

$$P_{cry}\% = \frac{1}{r_{tot}^3}\left(\frac{\sum_{i=1}^{n} P_i\% \cdot D_i}{2P_{cry}\%}\right)_{cry}^3 \times 100\,, \tag{4}$$

$$r_{tot}^3 = \frac{1}{P_{cry}\%}\left(\frac{\sum_{i=1}^{n} P_i\% \cdot D_i}{2P_{cry}\%}\right)_{cry}^3 \times 100\,. \tag{5}$$

If D_i is average diameter of polymer particles, Eq. (2) can be written as follows:

$$D_r = \sqrt[3]{\frac{\left(\dfrac{\sum_{i=1}^{n} P_i\% \cdot D_i}{P_{cry}\%}\right)^3}{P_{cry}\%}} \times 100\,. \tag{6}$$

The percentage of the crystals can be determined from XRD. By crystalline-peaks' parameters from Table 2, the particles' size can

be calculated by means of Eq. (6). The average particles' size is of 336.7 nm. The particles' size in this method may be closer to reality because the XRD includes a large number of particles and it is not optional as based on the SEM and AFM characterization.

3.6. Atomic Force Microscopy Analysis

Atomic force microscopy (AFM) is an excellent tool to study morphology and texture of diverse surfaces [28] and it is employed as a powerful technique to statistical study and analysis of the morphology of polymer thin films' surfaces with parameters such as roughness (R_a), root mean square (RMS), kurtosis (Ku), skewness (Sk) and mean diameter [29]. Atomic force microscopy scans the 5 μm×5 μm areas of polymer film with thickness of 280 nm.

Figure 7 shows 3D image, roughness, topography, mean diameter and elevation distribution of polymer film. Figure 7, *b* shows the polymer film roughness and RMS; statistical analysis of AFM data shows the surface parameter ($R_a = 2.63$ nm, $RMS = 23$ nm, $R_v = 2$ nm, $R_p = 34$ nm, $R_{\max} = 37$ nm, $Sk(RMS) = 1.98$ and $Ku = 5.49$), when polymer formed and precipitated, the active points in surface of substrate absorb polymer chains. They accumulate on surface, grow to join together and form a rough layer, which seems as joined balls. Figure 7, *d* shows mean diameter of polymer particles in film, where average size is of about 420 nm that corresponds to what the SEM images show in this work.

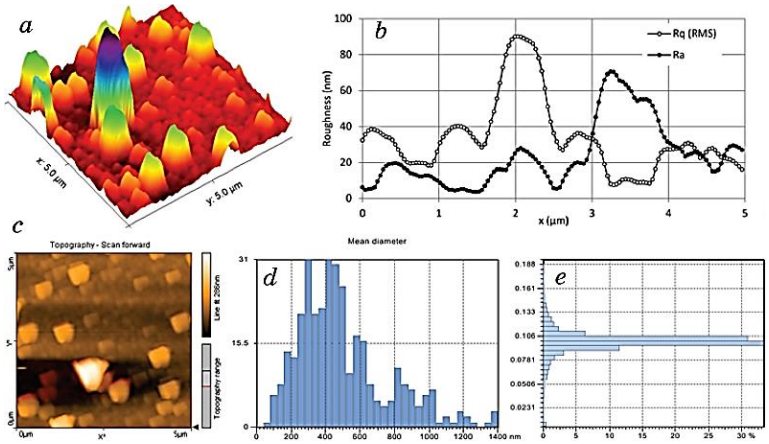

Fig. 7. *a*) 3D image; *b*) roughness; *c*) topography; *d*) mean diameter; *e*) elevation distribution of thin film of polymer.

4. CONCLUSIONS

A novel polymer was synthesized by a simple and easy method by adding concentrated hydrochloric acid to the monomer solution in alcohol. The polymer was characterized by FTIR, EDX, XRD and XPS to confirm its structure. The polymer was scanned by scanning electron microscope, and its film was investigated by AFM for its morphological properties. The polymer particles have a rough surface, its diameters were less than 1000 nm, and the average diameter was of about 430 nm (in the synthesis conditions). In XRD, the crystalline percentage $P_{cry}\%$ was of about 1.46%, and the average particles' size is of 336.7 nm.

5. HIGHLIGHTS

A novel polymer was synthesized and characterized by a simple and easy method.

New method was proposed for calculating polymer particles' size based on their crystallization and crystals' size from XRD data.

Particles' size determined by SEM and AFM is compared with XRD data.

6. COMPLIANCE WITH ETHICAL STANDARDS:

Funding. This study was funded by Al-Furat University and Damascus University.

Conflict of interest. Authors declare that they have no conflict of interest.

REFERENCES

1. R. Kumar, S. Singh, and B. C. Yadav, *IARJSET*, **2**, Iss. 11: 2394 (2015).
2. S. C. Hernandez, *Inter. Science*, **19**, Iss. 19–20: 2125 (2007).
3. Y. P. Zhang, S. H. Lee, K. R. Reddy, A. I. Gopalan, and K.P. Lee, *Journal of Applied Polymer Science*, **104**, No. 4: 2743 (2007); doi:10.1002/app.25938
4. A. Rudge, J. Davey, I. Raistrick, S. Gottesfeld, and J. P. Ferraris, *Journal of Power Sources*, **47**, Nos. 1–2: 89 (1994); doi:10.1016/0378-7753(94)80053-7
5. J. C. Zhang, X. Zheng, M. Chen, X. Y. Yang, and W. L. Cao, *Express Polymer Letters*, **5**, No. 5: 401 (2011); doi:10.3144/expresspolymlett.2011.39
6. A. Mirsakiyeva, *PhD Thesis* (Stockholm: KTH Royal Institute of Technology: 2017).
7. T. Kasa and F. Gebrewold, *Advances in Physics Theories and Applications*, **62**, No. 2017: 28 (2017).
8. L. Duan, J. Lu, W. Liu, P. Huang, W. Wang, and Z. Liu, *Colloids and Sur-*

faces A: Physicochemical and Engineering Aspects, **414**, No. 2012: 98 (2012); doi:10.1016/j.colsurfa.2012.08.033
9. G. Bayramoğlu, M. Karakışla, B. Altintaş, U. Metin, M. Saçak, and M. Arica, *Process Biochemistry*, **44**, No. 8: 880 (2009); doi:10.1016/j.procbio.2009.04.011
10. H. Gherras, A. Yahiaoui, A. Hachemaoui, A. Belfeda, A. Dehbi, and A. I. Mourad, *Journal of Semiconductors*, **39**, No. 10: 102001 (2018).
11. X. Ding, F. Tan, H. Zhao, M. Hua, M. Wang, Q. Xin, and Y. Zhang, *Journal of Membrane Science*, **570–571**, No. 1: 53 (2019); doi:10.1016/j.memsci.2018.10.033
12. G. H. Shim and S. H. Foulger, *Photonics and Nanostructures — Fundamentals and Applications*, **10**, No. 4: 440 (2012); doi:10.1016/j.photonics.2011.12.001
13. B. X. Valderrama, E. Rodríguez, E. G. Morales, K. M. Chane, and E. Rivera, *Molecules*, **21**, No. 172: 1 (2016); doi:10.3390/molecules21020172
14. R. Kumar, S. Singh, and B. C. Yadav, *International Advanced Research Journal in Science, Engineering and Technology*, **2**, Iss. 11: 110 (2015); doi:10.17148/IARJSET.2015.21123
15. D. Ateh, H. Navsaria, and P. Vadgama, *Journal of The Royal Society Interface*, **3**, Iss. 11: 741 (2016); doi:10.1098/rsif.2006.0141
16. W. Yuan, X. Yang, L. He, Y. Xue, S. Qin, and G. Tao, *Frontiers in Chemistry*, **6**, Iss. 1: 1 (2018); doi:10.3389/fchem.2018.00059
17. T.-H. Le, Y Kim, and H. Yoon, *Polymers*, **9**, Iss. 12: 150 (2017); doi:10.3390/polym9040150
18. R. Ansari, *E.-J. of Chem.*, **3**, Iss. 4: 186 (2006); doi:10.1155/2006/860413
19. Y. Shao, J. Wang, H. Wu, J. Liu, I. A. Aksay, and Y. Lin, *A Review. Electroanalysis*, **22**, Iss. 10: 1027 (2010); doi:10.1002/elan.200900571
20. D. Reynaerts, J. Peirs, and H. Van Brussel, *Sensors and Actuators A: Physical*, **61**, Nos. 1–3: 455 (1997); doi:10.1016/s0924-4247(97)80305-6
21. J. D. Larson, C. V. Fengel, N. P. Bradshaw, I. S. Romero, J. M. Leger, and A. R. Murphy, *Materials Chemistry and Physics*, **186**, No. 15: 67 (2017); doi:10.1016/j.matchemphys.2016.10.030
22. H. Braunling and R. Becker, *Basic Polypyrrylenemethines and Salts Thereof, and a Process for Their Preparation* (Patent No: US5004560A USA) (1991).
23. X.-Y. Hu, J. Ouyang, G. Liu, M. Gao, L. Song, J. Zang, and W. Chen, *Polymers*, **10**, No. 8: 882 (2018); doi:10.3390/polym10080882
24. S. B. Aziz, *Advances in Materials Science and Engineering*, **2016**, No. 1: 1 (2016); doi:10.1155/2016/2527013
25. A. S. Marf, R. M. Abdullah, and S. B. Aziz, *Membranes*, **10**, No. 4: 71 (2020); doi:10.3390/membranes10040071
26. B. Aziz, S. Marf, A. Dannoun, E. M. Brza, and R. M. Abdullah, *Polymers*, **12**, No. 10: 2184 (2020); doi:10.3390/polym12102184
27. C. He, C. Yang, and Y. Li, *Synthetic Metals*, **139**, No. 2: 539 (2003); doi:10.1016/s0379-6779(03)00360-6
28. B. Kumar and T. Rao, *Digest Journal of Nanomaterials and Biostructures*, **7**, No. 4: 1881 (2012).
29. J. Arjomandi, D. Raoufi, and F. Ghamari, *The Journal of Physical Chemistry C*, **120**, Iss. 32: 18055 (2016); https://doi.org/10.1021/acs.jpcc.6b04913